

AD-A167 698

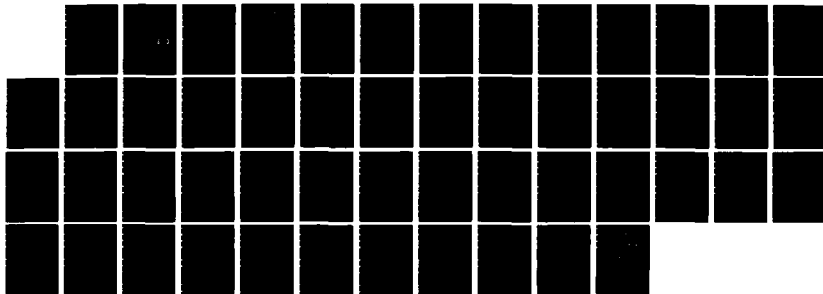
KINETICS OF SOME GAS PHASE ELEMENTARY REACTIONS OF
BORON MONOFLUORIDE (U) AEROSPACE CORP EL SEGUNDO CA
CHEMISTRY AND PHYSICS LAB G C LIGHT ET AL 81 APR 86
TR-0086(6945-84)-1 SD-TR-86-20

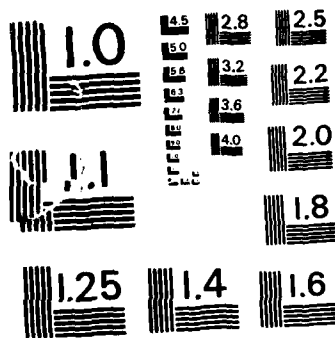
1/1

UNCLASSIFIED

F/G 7/4

NL





MICROCOPY RESOLUTION TEST CHART
NATIONAL BUREAU OF STANDARDS-1963-A

2

Kinetics of Some Gas Phase Elementary Reactions of Boron Monofluoride

G. C. LIGHT, R. R. HERM, and J. H. MATSUMOTO
Chemistry and Physics Laboratory
Laboratory Operations
The Aerospace Corporation
El Segundo, CA 90245

1 April 1986

DTIC
ELECTE
MAY 02 1986
S D
A

APPROVED FOR PUBLIC RELEASE;
DISTRIBUTION UNLIMITED

Prepared for
SPACE DIVISION
AIR FORCE SYSTEMS COMMAND
Los Angeles Air Force Station
P.O. Box 92960, Worldway Postal Center
Los Angeles, CA 90009-2960

AD-A167 690

OFF FILE COPY

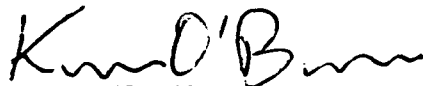
86 5 2 001

This report was submitted by The Aerospace Corporation, El Segundo, CA 90245, under Contract No. F04701-85-C-0086 with the Space Division, P.O. Box 92960, Worldway Postal Center, Los Angeles, CA 90009-2960. It was reviewed and approved for The Aerospace Corporation by S. Feuerstein, Director, Chemistry and Physics Laboratory.

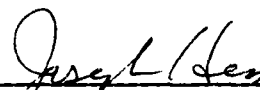
Capt Kevin O'Brien, SD/YNCS, was the project officer for the Mission-Oriented Investigation and Experimentation (MOIE) Program.

This report has been reviewed by the Public Affairs Office (PAS) and is releasable to the National Technical Information Service (NTIS). At NTIS, it will be available to the general public, including foreign nationals.

This technical report has been reviewed and is approved for publication. Publication of this report does not constitute Air Force approval of the report's findings or conclusions. It is published only for the exchange and stimulation of ideas.



KEVIN O'BRIEN, Capt, USAF
MOIE Project Officer
SD/YNCS



JOSEPH HESS, GM-15
Director, AFSTC West Coast Office
AFSTC/WCO OL-AB

UNCLASSIFIED

SECURITY CLASSIFICATION OF THIS PAGE (When Data Entered)

REPORT DOCUMENTATION PAGE		READ INSTRUCTIONS BEFORE COMPLETING FORM
1. REPORT NUMBER SD-TR-86-20	2. GOVT ACCESSION NO. AD-A167690	3. RECIPIENT'S CATALOG NUMBER
4. TITLE (and Subtitle) KINETICS OF SOME GAS PHASE ELEMENTARY REACTIONS OF BORON MONOFLUORIDE		5. TYPE OF REPORT & PERIOD COVERED
7. AUTHOR(s) Glenn C. Light, Ronald R. Herm, and James H. Matsumoto		6. PERFORMING ORG. REPORT NUMBER TR-0086(6945-04)-1
9. PERFORMING ORGANIZATION NAME AND ADDRESS The Aerospace Corporation El Segundo, Calif. 90245		8. CONTRACT OR GRANT NUMBER(s) F04701-85-C-0086
11. CONTROLLING OFFICE NAME AND ADDRESS Space Division Los Angeles Air Force Station El Segundo, Calif. 90009-2960		10. PROGRAM ELEMENT, PROJECT, TASK AREA & WORK UNIT NUMBERS
14. MONITORING AGENCY NAME & ADDRESS (if different from Controlling Office)		12. REPORT DATE 1 April 1986
		13. NUMBER OF PAGES 50
		15. SECURITY CLASS. (of this report) Unclassified
		15a. DECLASSIFICATION/DOWNGRADING SCHEDULE
16. DISTRIBUTION STATEMENT (of this Report) Approved for public release; distribution unlimited.		
17. DISTRIBUTION STATEMENT (of the abstract entered in Block 20, if different from Report)		
18. SUPPLEMENTARY NOTES		
19. KEY WORDS (Continue on reverse side if necessary and identify by block number) Boron Chemistry Reaction Chemistry		
20. ABSTRACT (Continue on reverse side if necessary and identify by block number) <div style="text-align: right;">(10 to the -11 power) (CC)</div> <p>Rate coefficients for some elementary bimolecular reactions involving the molecule BF have been measured in a gas phase flowtube facility. The BF + Cl₂ reaction was studied from 295 to 881 K. The rate coefficient is temperature independent with a value of $1.4 \pm 0.2 \times 10^{-11}$ cm³/molecule-sec. Reaction of BF with O₂ was studied between 675 and 1033 K. The inferred Arrhenius rate is $1.8 \times 10^{-11} \exp(-7240/T)$ cm³/molecule-sec. Room</p>		

DD FORM 1473
(FACSIMILE)

UNCLASSIFIED

SECURITY CLASSIFICATION OF THIS PAGE (When Data Entered)

UNCLASSIFIED

SECURITY CLASSIFICATION OF THIS PAGE (When Data Entered)

19. KEY WORDS (Continued)

20. ABSTRACT (Continued)

~~for -~~ ~~(10 to the -10 power)~~ ~~(10 to the -12 power)~~
temperature rate coefficients for $\text{BF} + \text{O}$ and $\text{BF} + \text{NO}_2$ were determined to be $1.8 \pm 0.4 \times 10^{-10}$ and $2.1 \pm 0.3 \times 10^{-13}$ ~~cm~~³/molecule-sec, respectively. Reaction of BF was undetectable upon mixing with H_2O , HF, CO_2 , NO, N_2O , SO_2 , or CH_3Cl . Upper limits are given for rate coefficients for these reactions. Boron monofluoride proved to be less reactive than other simple boron species which have been studied recently, namely, boron atoms and boron monoxide. Results for BF are compared with available rate information for reactions of isoelectronic CO and N_2 .

UNCLASSIFIED

SECURITY CLASSIFICATION OF THIS PAGE (When Data Entered)

CONTENTS

I.	INTRODUCTION.....	7
II.	APPARATUS AND EXPERIMENTAL PROCEDURE.....	11
	A. Flowtube and Gas Handling Systems.....	11
	B. UV Resonance Fluorescence Detection of BF.....	17
	C. Thermal Dissociation Source of BF.....	18
	D. Data Analysis Procedure.....	25
III.	RESULTS.....	27
	A. BF + O ₂	27
	B. BF + Cl ₂	31
	C. BF + NO ₂	33
	D. BF + O.....	35
	E. BF + NO, SO ₂ , HF, H ₂ O, CH ₃ Cl, CO ₂ , and N ₂ O.....	37
	F. BF + BF ₃	39
IV.	DISCUSSION.....	41
	REFERENCES	49

Accession For	
NTIS CRA&I	<input checked="" type="checkbox"/>
DTIC TAB	<input type="checkbox"/>
Unannounced	<input type="checkbox"/>
Justification	
By	
Distribution /	
Availability Codes	
Dist	Avail and/or Special
A-1	

TABLES

I.	BF + O ₂ Experiments Summary.....	29
II.	BF + Cl ₂ Experiments Summary.....	32
III.	BF + NO ₂ Experiments Summary.....	36
IV.	Estimated Addition Reaction Features.....	43
V.	Rates of Isoelectronic Reactions.....	46

FIGURES

1.	Schematics of Flowtubes for Geometries A and B.....	12
2.	Typical Data Comparing Temperature Readings Measured with Thermocouples on Outside Flowtube Wall and a Thermocouple Which Could be Slid Along the Axis of the Flowtube.....	16
3.	Schematic of $\text{BF}_3(\text{g}) + 2 \text{B}(\text{s}) \rightarrow 3 \text{BF}(\text{g})$ Resistively Heated Graphite Furnace.....	19
4.	Black Data Points, Joined by a Solid Curve, Measured at the Downstream End of the Flowtube as a Function of the Temperature of the Furnace.....	22
5.	Data Symbols Show BF Fluorescence Intensity Measured at Downstream End of the Flowtube as a Function of Partial Pressure of $\text{BF}_3(\text{g})$ at the Inlet of the BF Source Furnace.....	23
6.	Logarithm of Relative BF Fluorescence Intensity as Functions of Reaction Zone Length or Ratio of Reactant Density to Flow-Velocity Illustrate Typical Experimental Determinations of Rate Coefficients for the $\text{BF} + \text{O}_2$ Reaction by the Two Methods Discussed in the Text.....	28
7.	Plot of Different Determinations of Rate Coefficients of the $\text{BF} + \text{O}_2$ Reaction Listed in Table I as a Function of Reciprocal Temperature.....	30
8.	Typical Uncorrected and Corrected Relative BF Fluorescence Intensity Data as a Function of NO_2 Flowtube Density.....	34

I. INTRODUCTION

Boron binds strongly to oxygen and the halogens to form a variety of oxides, halides, and oxyhalides. Thus boron atoms, boron monoxide, and boron subhalides are capable of very exothermic abstraction reactions with a variety of oxidizing agents. Until recently, however, nothing was known about the rates of any of these reactions, except for some published estimated rate coefficients¹ and some indirect inferences provided by studies of the reaction of oxygen atoms with diborane and related species.² Starting in 1976, however, this situation changed dramatically with the report of the first of a series of measurements of chemiluminescence of boron atom reactions³⁻¹¹ and of rate coefficients for reactions of boron atoms,¹²⁻¹⁶ boron monoxide,¹⁷ and boron monofluoride.¹⁸ One scientific reason for this growing interest in elementary reactions of boron arises by virtue of its position in the periodic table as one of the lightest elements in that region between the families of good metals and nonmetals.^{6,9,13,18} Thus, the interest is to determine to what extent the reaction dynamics of boron atoms and its simple compounds can be interpreted in terms of reaction mechanisms which are typical of the metals or of the nonmetals.

This report presents results of a flow tube study of the rates of some reactions of boron monofluoride; a preliminary report of some of this work was given in Ref. 18. Temperature dependent rate coefficients are reported for the reactions



where the heats of reaction in kJ/mole are taken from the JANNAF tables. A rate coefficient at room temperature is reported for



Finally, upper limits to the rate coefficient at room temperature are reported for



In addition, an upper limit has also been measured at $T = 998\text{K}$ for Reaction (5), and some qualitative observations are reported on the reaction of BF with BF_3 . The quantity actually measured here is the pseudo-first order removal of

the molecule BF by reaction from which the rate constant is deduced. The reactions written here indicate the most exothermic product channel, but no measurements were made to verify that this was the product formed. Thus, there are other exothermic product channels for some of these reactants so that the actual reaction might not be as written here. In particular, Reaction (1) could also produce $\text{BO}_2 + \text{F}$ with an exothermicity of $\Delta H_{298}^\circ = -90$ kJ/mole.

Prior to this study, very little was known about the chemistry of BF. Thermodynamic calculations indicate that BF_3 gas may be quantitatively converted to BF gas upon passage over hot boron powder, and free energies of formation of gaseous BF were originally measured by this thermal transpiration technique.¹⁹ It was subsequently employed by Timms²⁰ in one of the pioneering studies of synthesis by condensation of a high temperature vapor with other reagents. However, Timms²⁰ found that the useful synthesis reactions of BF were limited to insertion into other BF bonds and addition across double and triple organic bonds. Additional qualitative indications were provided by Moeller and Silvers²¹ who produced BF by a microwave discharge in BF_3 and reported that it was very long-lived when mixed with helium in their flow apparatus.

II. APPARATUS AND EXPERIMENTAL PROCEDURE

A. FLOWTUBE AND GAS HANDLING SYSTEMS

The reactions were studied in flowtubes shown in Fig. 1 as geometries A and B. Geometry A was used for all of the reactions which were studied only at room temperature, 294K. Geometry B was employed in the temperature-dependent studies, viz. O_2 , Cl_2 , and some measurements with H_2O . The BF source and UV resonance fluorescence detector, discussed below, were common to both geometries.

Both flowtubes were fabricated of fused quartz tubing of 2.5 cm inside diameter. The inside walls were initially cleaned with ammonium bifluoride, rinsed with distilled water, and baked at 473 K except for the studies with HF discussed later. Flow rates of all gases entering the flowtubes were measured directly either with calibrated Matheson rotameters or, in the case of most of the reactants, by the rate of pressure drop in a supply vessel of known volume. Total gas pressure in the flowtube was measured by a 0-20 Torr Wallace and Tiernan bourdon tube gauge.

For geometry A, the outside of the flowtube was exposed directly to room air over its entire length. The reaction zone length was fixed at 87.5 cm and was defined by the end of the injection tube for BF at its upstream end and by the center of the fluorescence cell at the downstream end. The reactant gas was introduced in an excess of inert nitrogen carrier gas from a side arm at a point 15 cm upstream from the BF injector. Measurements of rate coefficient were made by varying the reactant flow rate by means of a variable leak valve.

For the measurements of reaction with O, atomic oxygen was provided by partial titration with NO in the

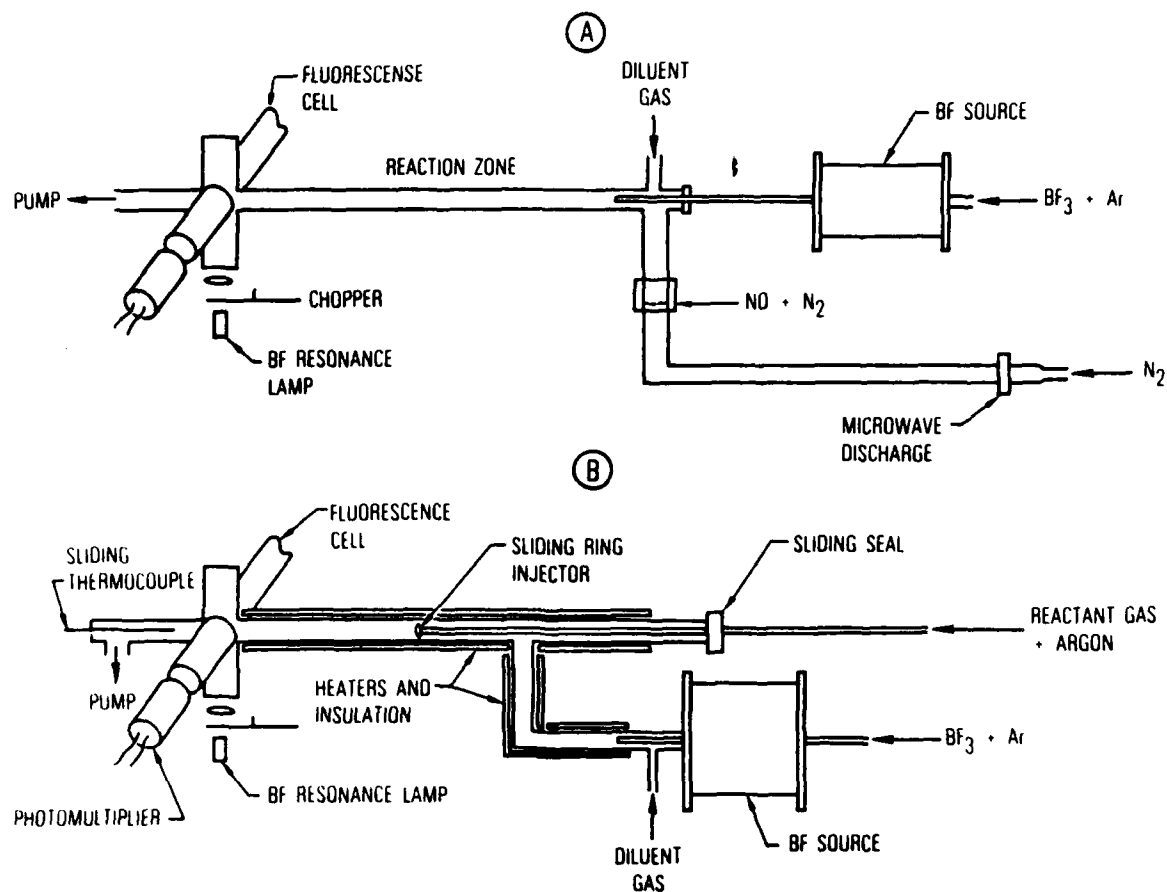


Fig. 1. Schematics of Flowtubes for Geometries A and B



(12)

reaction for which the nitrogen atoms were generated in a microwave discharge in Matheson UHP grade N_2 , as shown in Fig. 1. The residence time of the nitrogen flow between the microwave discharge and the NO inlet exceeded one second in order to ensure relaxation of metastable states of N and N_2 . The nitric oxide was taken from a cylinder and purified by three repetitions of a trap-to-trap distillation and pump-off procedure using traps at 77K and 196K. It was then admitted to the side arm of the flowtube through an injector designed to promote mixing of gas flows. The rate data were collected with reaction (12) undertitrated, so that the density of O in the reaction zone was given directly by the flow rate of NO, after first ascertaining that addition of active nitrogen itself had no influence on the BF density for the experimental conditions employed.

For the other reactants used in geometry A, the microwave power was turned off and the reactant of interest was substituted for NO. For most of the other reactants in geometry A, no special handling or purification was required, and the gases were taken from pressurized cylinders of the pure gas. This includes CO_2 , N_2O , CH_3Cl , and SO_2 ; NO_2 is discussed later. When NO was the reactant, the same purification procedure described above was used. In the case of H_2O , the source volume received the vapor at 4 Torr partial pressure from a Pyrex container of degassed distilled liquid water held at 273 K by an exterior water-ice slush. This was then diluted with argon. The leak valve was wrapped with heating tape and heated to 473K while data were obtained in order to prevent condensation associated with the pressure drop through the orifice.

In the case of HF, a number of changes were made to prevent unwanted chemical removal of the reactant. The Pyrex source volume was replaced with a stainless steel sample cylinder. All of the interior quartz surfaces of the flowtube which would experience contact with HF, including the fluorescence cell, were coated with halocarbon wax. All of the source volume upstream of the variable leak valve, including the stainless steel sample cylinder, was passivated by exposure to HF.

For geometry B, the reaction zone of the flowtube was heated by five contiguous separately controlled resistive heating elements embedded in split cylinder ceramic holders with inside diameter of 3.2 cm. In addition, the ceramic holders were enclosed in multiple layers of ceramic fiber blanket for thermal insulation. The reaction zone was defined at its upstream end by a multiply-perforated sliding quartz ring injector where the reactant gas was admitted to the flow. Thus the reaction zone length was variable up to a maximum of 53 cm by sliding the ring injector along the flowtube. The side arm carrying BF from the furnace and the main flowtube upstream of the side arm connection were both also heated for a distance of 35 cm to ensure that the gas temperature in the reaction zone was uniform.

There were five Pt-Pt-Rh thermocouples positioned along the reaction zone in the annular space between the heaters and the flowtube and two thermocouples along each of the preheated sections of the flowtube; these are not shown in Fig. 1. In preparation for obtaining measurements at an elevated temperature, power to each heater was adjusted until all of the nine thermocouples indicated the same temperature. During the measurement, the thermocouple readings along the reaction zone were allowed to vary by no more than ± 10 degrees about the mean. The significance of this variation for the accuracy of the rate measurements depends on the temperature dependence of the

reaction rate in question and was found after the fact to be insignificant for Reaction (1).

In addition to these temperature measurements, the flowtube gas temperature was measured directly using a doubly shielded thermocouple²² which was positioned on the axis of the flowtube and could be translated to any axial position along the reaction zone. To preclude the possibility of erroneous data from catalytic effects on the thermocouple surface, measurements of gas temperature with this device were made with only inert carrier gas flowing, without reactant and BF_3 flow, and with the BF source furnace and flowtube wall heaters turned on. When reaction rate data were being obtained, this thermocouple was withdrawn from the flowtube.

An example of data for the axial distribution of gas temperature measured with this doubly shielded thermocouple is shown in Fig. 2. Westerberg²³ has shown that a region of temperature gradient such as shown here has no effect on data for reaction rate collected by varying the reaction zone length in the constant temperature region. Reaction rate coefficient determinations, presented later, show no significant differences between data on Reaction (1) obtained by varying the reaction zone length in the isothermal section of the flowtube with constant O_2 density and by varying the O_2 density at constant length. Using the variable reactant density method, the problem presented by the region of temperature gradient reduces to an appropriate choice of reaction zone length, estimated as an uncertainty of ± 2 cm or an uncertainty in measured rate of about $\pm 4\%$. In the case of Cl_2 , the only other reactant for which data were obtained at elevated temperature, the reaction is essentially temperature independent.

As discussed in Ref. 22, there are often differences between the indicated temperatures of shielded and unshielded thermocouples in flowtubes

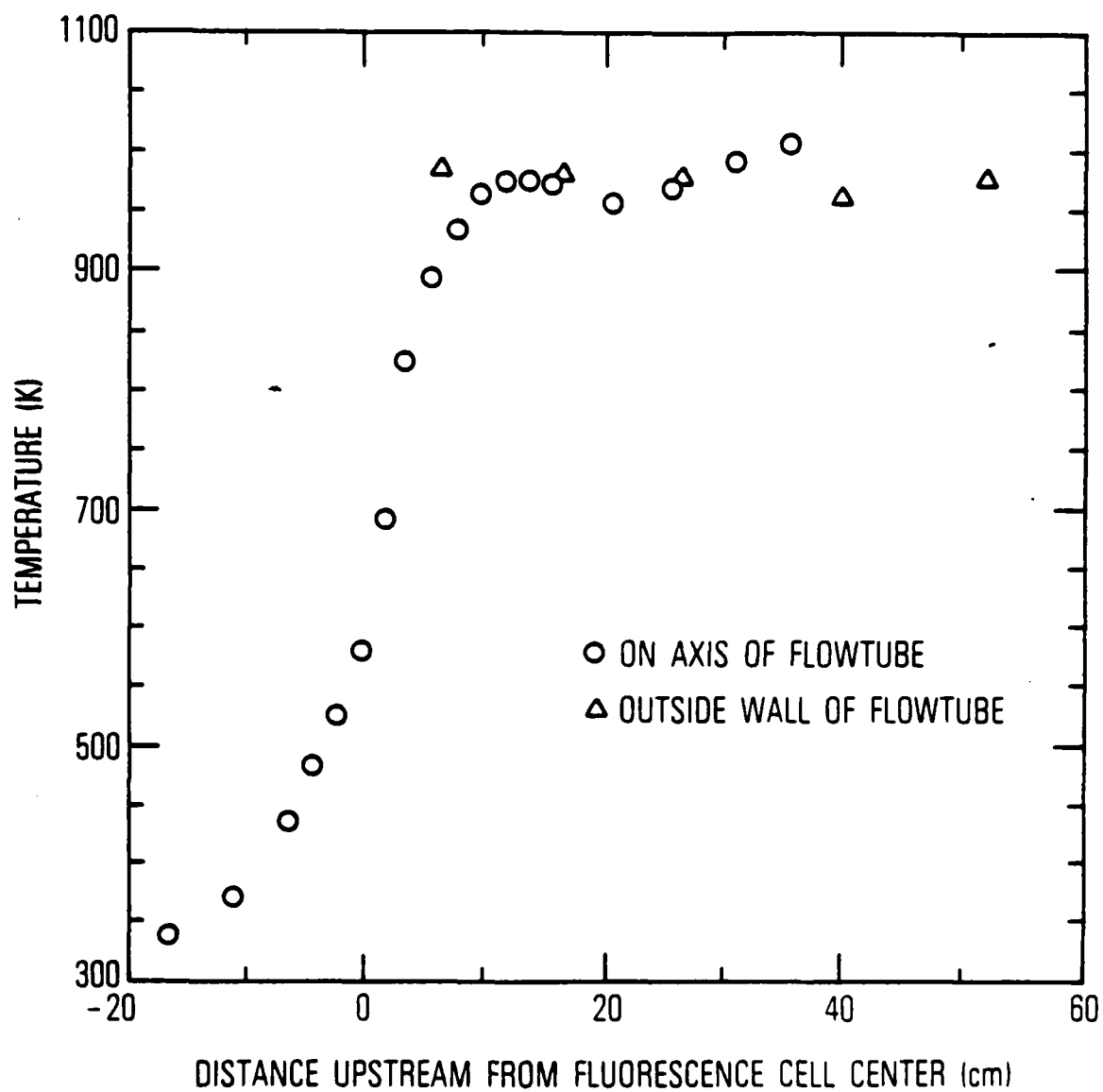


Fig. 2. Typical Data Comparing Temperature Readings Measured with Thermocouples on Outside Flowtube Wall and a Thermocouple Which Could be Slid Along the Axis of the Flowtube

owing to radiative transfer with nearly opaque surfaces. Small differences ($\Delta T < 20K$) were noted in this work between the readings from the shielded thermocouple in the flow and those outside the flowtube between the flowtube and the heater ceramic surface. These small differences were inconsequential in the studies reported here.

B. UV RESONANCE FLUORESCENCE DETECTION OF BF

Relative BF density at the end of the reaction zone was determined by means of resonance fluorescence in the ($A^1\Pi \rightarrow X^1\Sigma$) BF band system with a 0-0 band at 196 nm. The light source was a microwave discharge in BF_3 in an excess of either helium or argon carrier gas, similar to that used by Moeller and Silvers.²¹ The emission spectrum of the lamp was similar to that reported in Ref. 21. The only discernible spectral structure other than those attributable to the $A^1\Pi \rightarrow X^1\Sigma$ transition in BF were the two boron atom resonance doublets at 208.9 and 249.7 nm.

The lamp was constructed of fused quartz except for the output window which was surrasil grade fused quartz. The fluorescence cell was formed of fused quartz in the shape of a cross fused at right angles to the main flowtube. The arms of the cross were 50 mm inside diameter. The lamp light entrance window and the fluorescence exit window were each 11.4 cm from the flowtube axis and had a clear aperture of 1.8 cm. Light from the resonance lamp was brought to a focus near the flowtube axis, and the fluorescence emitted perpendicular was detected. Multiple circular knife edge baffles in the lamp light entrance arm and in the fluorescence exit arm served to reduce the background scattered light reaching the EMI 9635QB photomultiplier tube detector.

The resonance lamp output was chopped at 200 Hz, and the fluorescence was synchronously detected on a PAR 124A lock-in amplifier. The best fluorescence signal dynamic range was achieved with the use of a pair of band pass interference filters* positioned in front of the photomultiplier tube. Combined transmission of the filter pair was 14% at 195 nm with a FWHM bandpass of 4 nm. Transmission at the wavelengths of boron atom lines present in the lamp output was 1% at 208.9 nm and about 0.1% at 249.7 nm.

A flow of argon sweeper gas was maintained in each of the four arms of the fluorescence cell in the direction away from the windows in order to prevent collection of any condensed reaction products on the cell windows. The total sweeper gas flow rate was about 10% of that in the flowtube.

C. THERMAL DISSOCIATION SOURCE OF BF

Boron monofluoride was generated by the reaction of BF_3 gas with solid boron at elevated temperature in a resistively heated graphite tube in a manner similar to that of Blauer¹⁹ and Timms.²⁰ A schematic of the source appears in Fig. 3. Here, BF is made in the reaction



by flowing BF_3 in an excess of argon carrier gas over granules of crystalline boron at a temperature in the range of 1770 to 1880K. The graphite tube had inside and outside diameters of 0.63 and 1.27 cm respectively; the hot central portion was 12 cm long. The tube was fabricated from POCO graphite with a thin outer coating of pyrolytic graphite to reduce the porosity. It was supported at both ends by water cooled copper clamps which also served as electrical connections. Electrical current at 60 Hz and cooling water were

*Purchased from Acton Research Corporation, 525 Main St.,
Acton, Mass. 01720

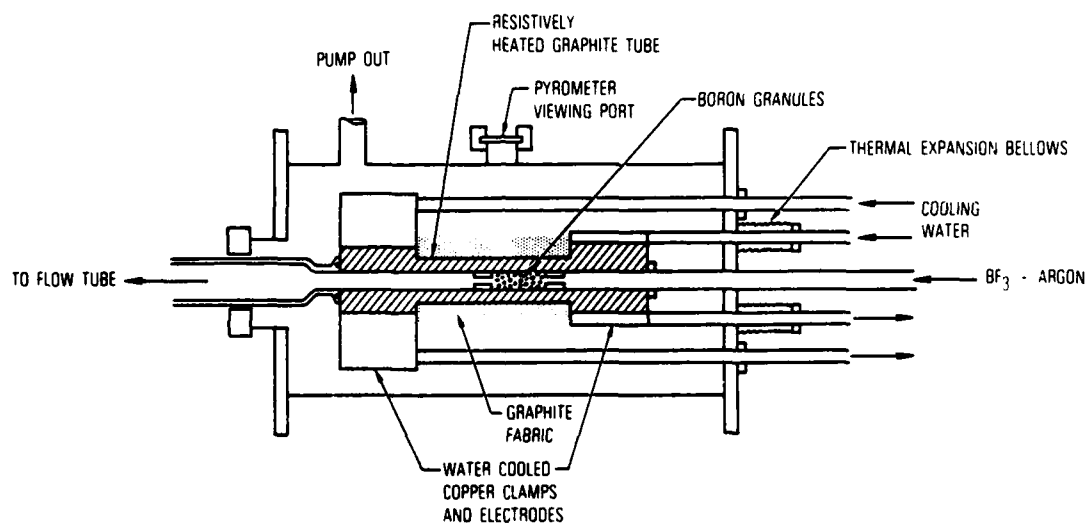


Fig. 3. Schematic of $\text{BF}_3(\text{g}) + 2 \text{B}(\text{s}) \rightarrow 3 \text{BF}(\text{g})$ Resistively Heated Graphite Furnace. The vacuum jacket was maintained at $\sim 1\text{-}10 \mu\text{m}$ by means of a small mechanical oil pump.

brought through the vacuum vessel walls to the copper clamps by hollow copper rods. The graphite tube was wrapped with several layers of graphite fabric for insulation. Furnace temperature was determined by an optical pyrometer viewing the central portion of the graphite tube through a hole in the insulation and a window in the vacuum vessel. Thermal expansion and contraction of the graphite rod was accommodated by stainless steel expansion bellows in the vacuum seal on two of the four copper rods which supported the graphite tube.

The solid boron consisted of pieces no more than 0.6 cm in largest dimensions and of purity stated by the vendor to be > 99.8%. The column of boron pieces was held in place in the furnace by hollow cylindrical graphite ferrules, 1.27 cm long and 0.3 cm inside diameter. The BF_3 vapor was taken directly from a cylinder purchased from Matheson with stated purity of 99.5%. The flow rate of BF_3 into the furnace was controlled by a variable leak valve and determined from the rate of pressure decrease in a source vessel of known volume measured with a calibrated Pace transducer. Materials in contact with the BF_3 in the source vessel consisted of stainless steel, Pyrex glassware, one rubber O-Ring, and the materials within the Granville-Phillips Model 203 Variable Leak Valve. In order to operate with measurable rates of pressure decay and still have an appropriate BF_3 flow rate and usable running time, it was necessary to dilute the BF_3 in the source vessel by about a factor of 50 with an excess of argon. Before entering the furnace, the BF_3 was further diluted by a very large excess of argon at a point immediately downstream of the variable leak. Under all conditions this argon formed the greatest part of the flow in the system. The ratio of the total flow rates of argon and BF_3 was typically of order 10^5 . All of the argon used was Matheson UHP grade, and it was further purified to less than 0.1 ppm oxygen and water vapor by passing through a Matheson Model 8301 Hydrox Purifier.

In order to characterize the performance of the furnace source, measurements were made of BF fluorescence, detected at the downstream end of the flowtube, as a function of furnace temperature and of BF_3 input flow rate. The results are shown in Figs. 4 and 5 and are compared with the expected behavior based on thermodynamic equilibrium within the furnace, although equilibrium might not be realized due to kinetic limitations. In Fig. 4, data are more or less uniformly displaced from the expected curve to higher temperatures. This suggested that the temperature inside of the furnace might be uniformly shifted by a constant amount to a temperature lower than that of the outside furnace wall. This could result from the flow of inert diluent gas through the oven cooling the surfaces which it contacts, imposing a flow rate dependent temperature difference between the internal gas flow and the external graphite surface. This interpretation was qualitatively verified subsequent to obtaining the data on BF production shown here by employing two optical pyrometers simultaneously. Here, one viewed the external graphite surface, as previously described, and the other viewed the interior of the furnace in the direction of its cylindrical axis from the downstream side. If Fig. 4 is interpreted to mean that the effective flow temperature is lower than the pyrometer measurement by $\sim 232\text{K}$, the comparison in Fig. 5 shows that the fluorescence signals correlate nicely with the calculated BF production rate.

Further evidence was obtained which showed that neither gas phase atomic boron nor entrained particulate matter could be responsible for a significant fraction of the detected signal. This was obtained by separately placing two different filters between the resonance lamp and the fluorescence cell. When a filter was used which transmitted radiation from the boron atom resonance doublet at 249.7 nm and substantially rejected the BF system at 195.7 nm , no

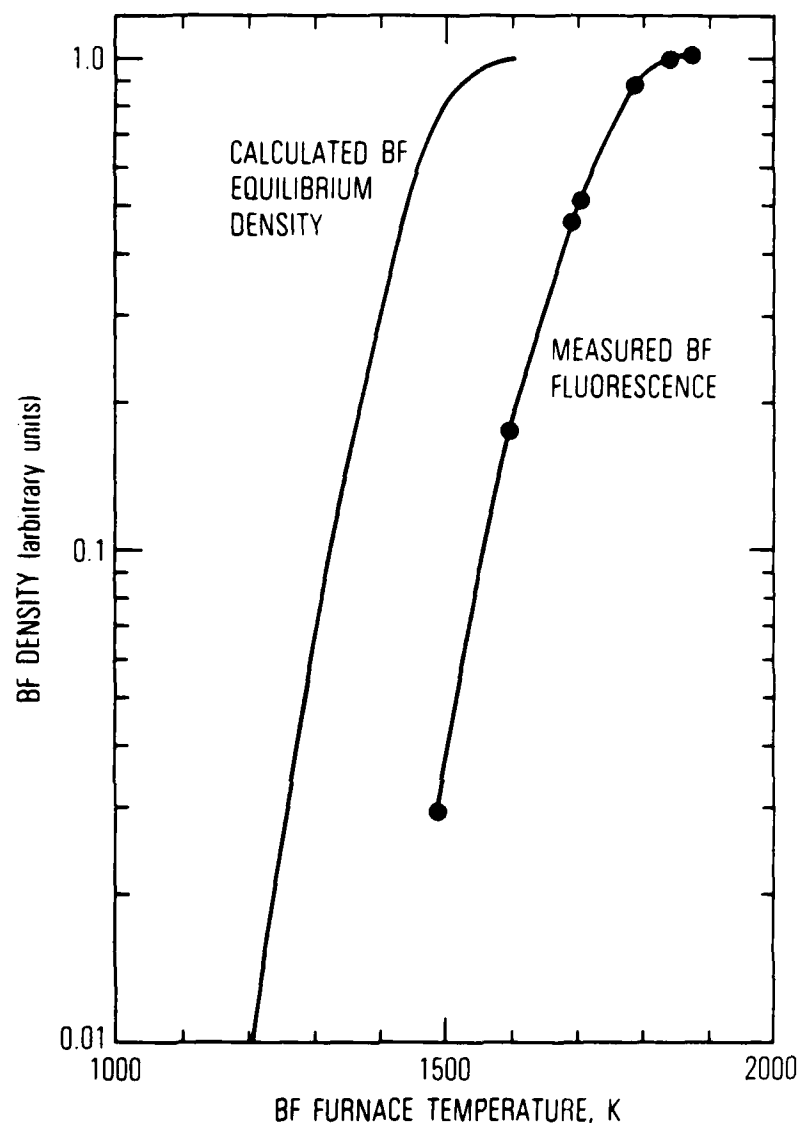


Fig. 4. Black Data Points, Joined by a Solid Curve, Measured at the Downstream End of the Flowtube as a Function of the Temperature of the Furnace. The temperature was read from a pyrometer viewing the outer wall of the graphite furnace through the viewing port shown in Fig. 3. All data were recorded for fixed gas flow rates into the furnace of 0.043 moles argon/min and 5.6×10^{-8} moles BF_3 /min and a flowtube pressure of 2.3 Torr. The other solid curve shows the temperature variation of the calculated $\text{BF}_{(g)}$ pressure for thermodynamics equilibrium with $\text{BF}_{3(g)}$ and $\text{B}_{(s)}$, Reaction (13), for this $\text{BF}_{3(g)}$ starting condition. The two curves were normalized to the same high temperature asymptotic BF density limit.

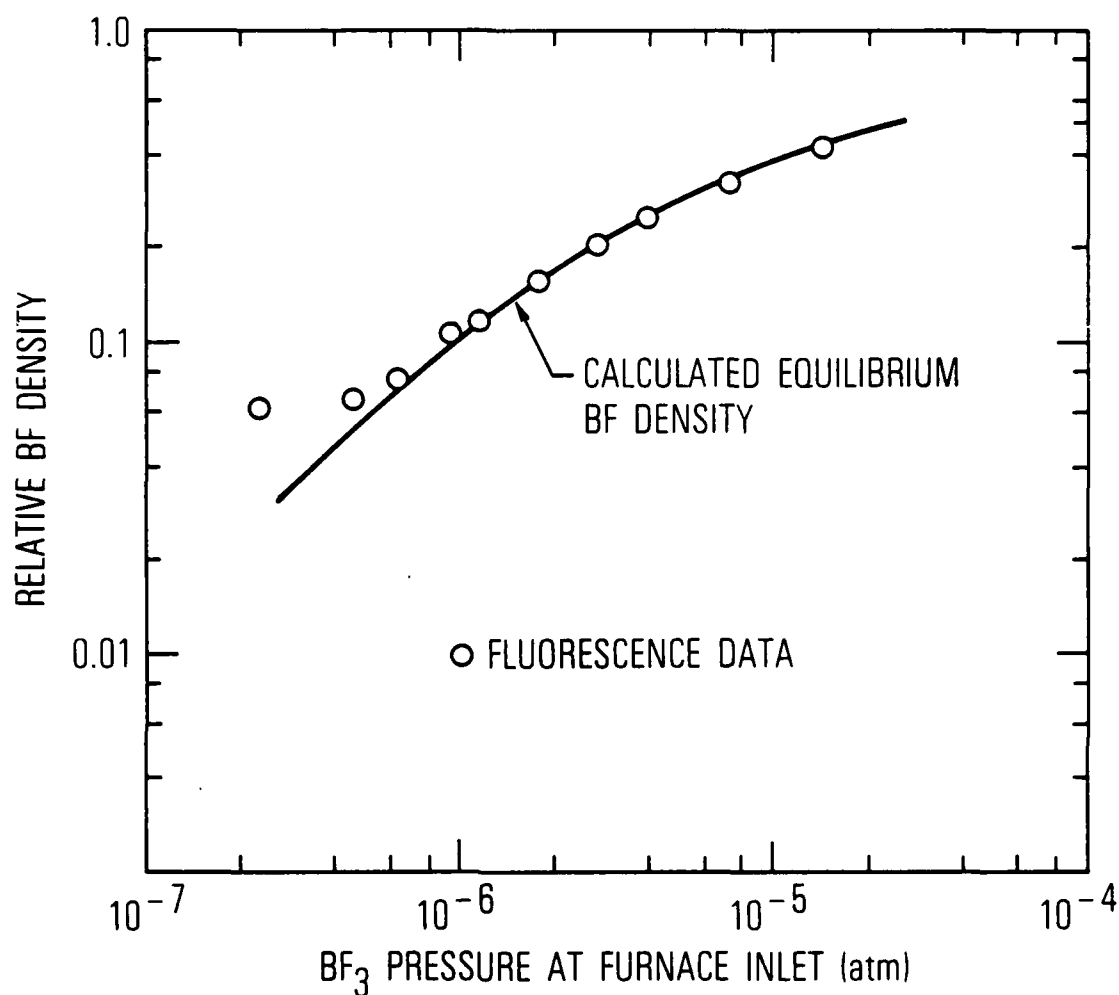


Fig. 5. Data Symbols Show BF Fluorescence Intensity Measured at Downstream End of the Flowtube as a Function of Partial Pressure of $\text{BF}_3(\text{g})$ at the Inlet of the BF Source Furnace. Argon diluent gas was used to maintain a total pressure in the flowtube of 0.8 Torr. Furnace temperature, measured with pyrometer viewing its outer wall, was 1793 K. The solid curve, normalized to the data points, indicates the calculated BF density in equilibrium with $\text{B}(\text{s})$ and $\text{BF}_3(\text{g})$ within the furnace for an assumed interior furnace temperature of 1561 K, corresponding to the 232 K displacement from the measured temperature shown in Fig. 4.

fluorescence was observed. On the other hand, the fluorescence was reduced by just the transmission coefficient of the filter at 195.7 nm when a filter was used which rejected both boron atom resonance doublets at 208.9 nm and 249.7 nm but passed the BF system at 195.7 nm.

These observations are all consistent with the interpretation that the resonance fluorescence signal is proportional to the density of BF molecules in the flowtube. This is certainly the expected behavior since: (1) the BF furnace temperatures are too low to expect any appreciable vaporization of boron atoms; (2) there is no reason to expect an entrainment of particulates in the flow which would be dependent on the furnace temperature; and (3) the input flow rate of BF_3 was always very small. This latter condition was necessary to ensure negligible contribution from possible nonlinearities at higher BF_3 flow rates, such as significant absorption of the BF resonance radiation or electronic quenching of $\text{BF}(^1\Pi)$ by boron fluoride species in the fluorescence cell. Nevertheless, an estimate of the absolute intensity of the resonance lamp and of fluorescence and detection efficiencies indicated that the observed resonance fluorescence signals were much weaker than would be expected if all of the BF_3 were converted to BF and if BF loss at the walls were negligible.

All of this supports an interpretation wherein BF_3 is quantitatively converted into BF within the furnace but most of the BF is lost between the furnace source and the fluorescence detector. This is of no consequence to the interpretation of the kinetics measurements since knowledge of the absolute density of BF is not required and since the inferred rate coefficient is insensitive to the occurrence of a wall loss rate and possible production of other boron fluorides. Initially, however, this appeared to conflict with other observations^{21,24} suggesting inconsequential wall losses of BF in a room

temperature flowtube. However, some further observations appeared to remove the apparent conflict and indicated negligible loss on room temperature walls but significant loss on higher temperature walls.

D. DATA ANALYSIS PROCEDURE

All data was collected with a BF density much less than that of its co-reactant so that the BF density followed the usual pseudo-first order decay,

$$\ln ([BF]/[BF]_0) = - \frac{\epsilon k z}{\bar{v}} [A] \quad (14)$$

where $[A]$ is the density of the co-reactant, z is the length of the reaction zone, \bar{v} is the average gas flow velocity through the reaction zone, and k is the quantity of interest, the bimolecular reaction rate coefficient. Except for isolated complications due to changing \bar{v} or to fluorescence of co-reactant A which are discussed under data for individual reactions, the ratio of BF densities in the presence and absence of reaction, $[BF]/[BF]_0$, was given by the corresponding ratio of measured BF resonance fluorescence intensities. As discussed in Ref. 18, this is true because collisional quenching of the $A^1\Pi$ electronic state of BF by co-reactant A was negligible by virtue of the very short radiative lifetime of the $A^1\Pi$ state. Here, ϵ is a term which is always in the range $0.62 < \epsilon < 1.0$ and which accounts for any radial gradient in the concentration of BF brought about by the combined effects of the parabolic velocity profile, gas phase chemical removal of BF in the reaction of interest, and loss of BF at the wall. The analysis of Poirier and Carr²⁵ was used in this work to evaluate the magnitude of ϵ for each data point in the process of data analysis. For this purpose, the wall loss rate was ignored. This is known to be incorrect for the higher reaction temperatures, but its

effect on inferred rate coefficients is negligible. In most of the data, this correction was found to be negligible and ϵ was close to unity. Other effects due to axial pressure gradient and BF diffusion were always negligible.²⁶

The gas velocity \bar{v} was determined from the measured total gas flow rate F_T , the flowtube cross sectional area, and the measured pressure and temperature in the reaction zone. These data are given for the different reactions in the next Section, and the resultant range in \bar{v} is shown for BF + O₂ as an example. The density of the co-reactant, [A], was evaluated from the ratio of its measured flow rate, F_A , to the total flow rate and the known pressure and temperature in the reaction zone. With the exception of some of the studies of Reaction (1) discussed later, all data were collected with a great excess of inert carrier gas, argon or helium, so that $F_T \gg F_A$ and changes in F_A produced negligible change in \bar{v} or total pressure in the reaction zone. In geometry A, rate coefficients were determined from Eq. (14) with [A] as the parameter which was varied during an experiment. In geometry B, rate coefficients were determined with either [A] or z as the parameter which was varied during an experiment. A rate coefficient was deduced from the slope of a straight line fitted to the data for $\ln ([BF]/[BF]_0)$ vs $\frac{\epsilon[A]}{\bar{v}}$ or $\frac{\epsilon z}{\bar{v}}$, as appropriate, using the method of least squares. When the independent variable was co-reactant density, this line was constrained to pass through the origin. When the independent variable was reaction zone length, it was not so constrained because of small uncertainty about the reaction zone dimension.

Reported rate coefficients are presented with 95% confidence limits based on random errors in the measurements. Possible additional systematic errors are believed to be small, $\sim 10\%$.

III. RESULTS

A. BF + O₂

Data for the rate of the reaction of BF with O₂ were obtained for reactant temperatures in the range 675 < T < 1033K using the flowtube geometry

B. Data were obtained by both the variable reactant density method and the variable reaction zone length method using argon as the inert diluent gas in all cases. An example of the data for each type is shown in Fig. 6. Table I presents the conditions of measurement and the deduced rate coefficients for the different experimental runs. Data for the temperature dependent rate constant are summarized in Fig. 7. The fitted Arrhenius rate expression is

$$k_1 = 1.8 \times 10^{-11} \exp(-7240/T), \text{ cm}^3/\text{molecule-sec.} \quad (15)$$

For data obtained at the lower temperatures using the variable reactant density method only, corrections of two kinds were applied in the course of data analysis. For some of the data, the amount of oxygen added to the flow to bring about a measurable reaction rate was sufficient to slightly increase the flowtube pressure and thus change the velocity \bar{v} . Because of the small change in flow conditions with added O₂, the experimentally determined ratio, $\ln ([\text{BF}]/[\text{BF}]_0)_M$, also had to be corrected. In effect for these data, the measured ratio of fluorescence signals obtained with and without added oxygen contains contributions from both the chemical removal of BF in the reaction of interest as well as from the changed flow conditions. The appropriate corrections were determined from the separately measured dependence of fluorescence signal on argon flow rate. For these measurements, only the flow of argon through the reactant sliding injection was varied. The assumption

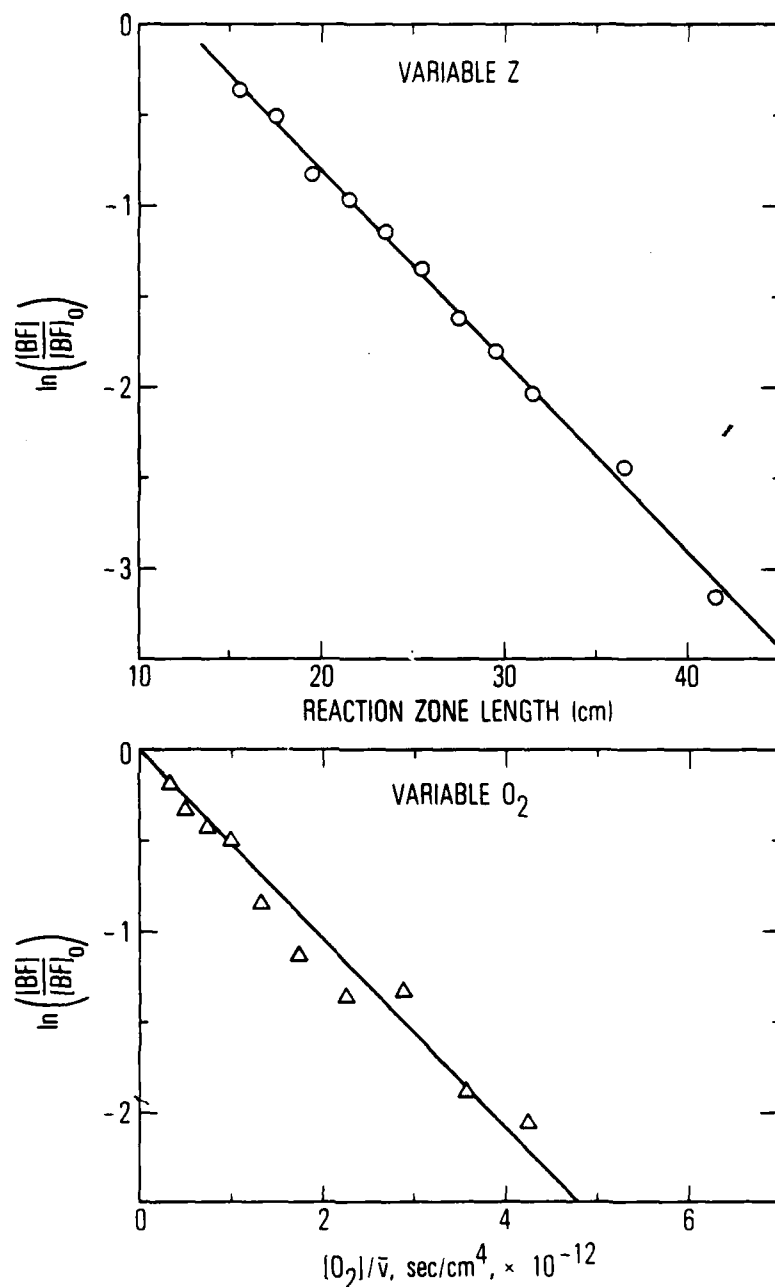


Fig. 6. Logorithm of Relative BF Fluorescence Intensity as Functions of Reaction Zone Length or Ratio of Reactant Density to Flow-Velocity Illustrate Typical Experimental Determinations of Rate Coefficients for the $BF + O_2$ Reaction by the Two Methods Discussed in the Text. Data plotted are for the last two entries in Table I, i.e., temperatures of 994 and 989 K, respectively.

Table I. BF + O₂ Experiments Summary

Reaction Temperature K	Gas Flow Rates ^a		Pressure Torr	Average Gas Velocity ^b (cm/sec)	Parameter Varied	Rate Coefficient ^c k ₁
	10 ⁵ F _{BF₃}	F _T				
1033	1.1	1.2	5.5	1820-1860	[O ₂]	18 ± 1.5
675	1.8	1.1	6.0	1030-1060	[O ₂]	0.43 ± 0.13
813	0.59	1.1	6.0	1220-1270	[O ₂]	2.7 ± 0.21
784	0.90	1.1	6.1	1150-1210	[O ₂]	1.9 ± 0.08
787	0.90	2.2	10.1	1340-1380	[O ₂]	1.6 ± 0.10
876	2.1	1.1	6.1	1250-1310	[O ₂]	3.8 ± 0.23
873	0.16	2.3	10.7	1490-1520	[O ₂]	4.4 ± 0.10
881	0.33	1.1	6.8	1320-1390	[O ₂]	5.2 ± 0.10
881	2.8	1.1	6.8	1320-1390	[O ₂]	5.3 ± 0.18
885	0.35	1.3	6.8	1390	z	4.2 ± 0.44
988	0.80	1.1	6.0	1480-1550	[O ₂]	12 ± 0.50
986	3.0	1.1	6.0	1450-1520	[O ₂]	10 ± 0.70
988	3.0	1.1	6.9	1520	z	13 ± 2.6
989	0.16	2.0	10.9	1460-1490	[O ₂]	12 ± 1.0
989	0.16	2.0	10.9	1410-1440	[O ₂]	12 ± 1.0
994	0.21	2.3	12.0	1490	z	14 ± 0.70

^a F_{BF₃} and F_T are flow rates in standard (273K and 760 Torr) liters/min of BF₃ and total gas, respectively.

^b Minimum and maximum values are shown when variable [O₂] method was used (see text)) and the single value is shown when variable z method was used.

^c The bimolecular rate constant, k₁, calculated from a fit of Eq. (14) to each data set listed, is given in units of 10⁻¹⁵ cm³/molecule-sec.

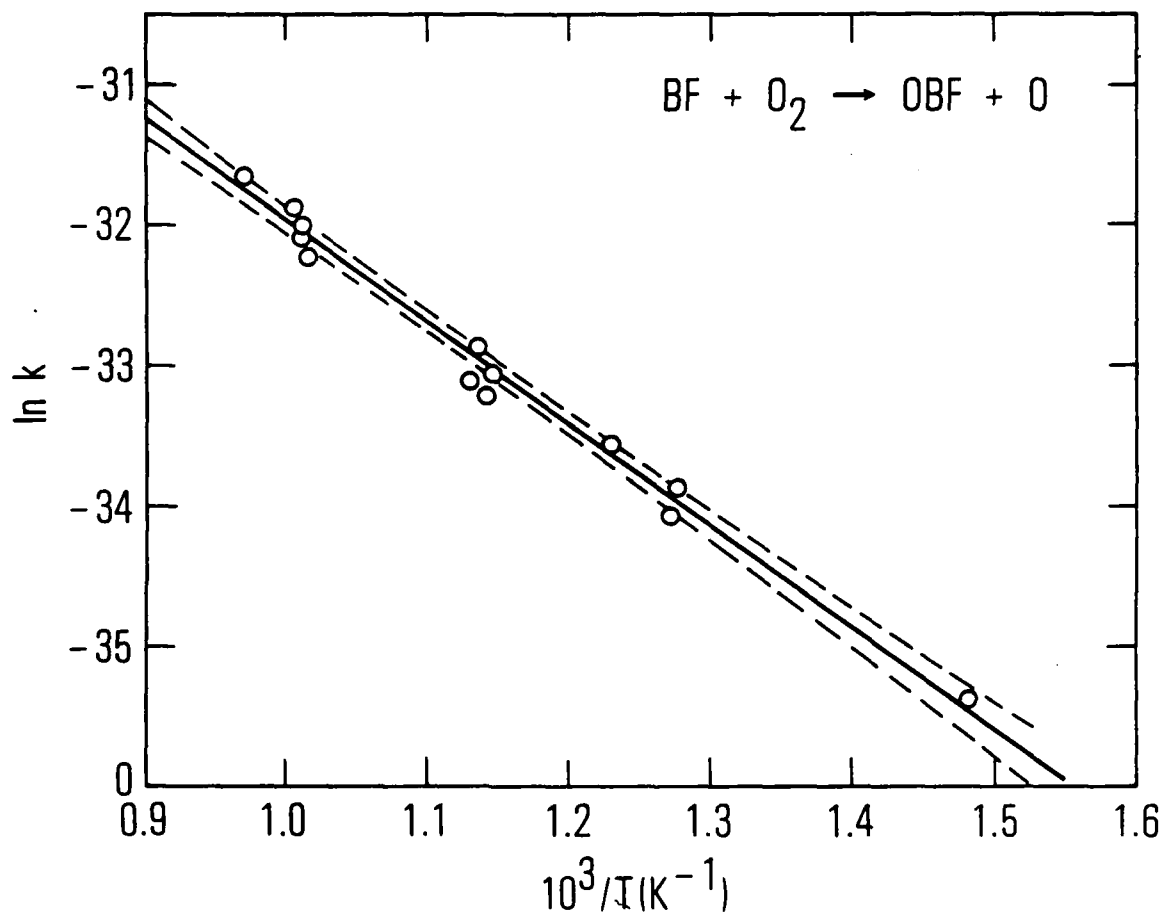


Fig. 7. Plot of Different Determinations of Rate Coefficients of the $\text{BF} + \text{O}_2$ Reaction Listed in Table I as a Function of Reciprocal Temperature. Solid line shows best Arrhenius rate expression fit to this data, Eq. (15). Dashed lines show the calculated 95% confidence limits on the fitted rate expression.

implicit in this procedure is that the change in fluorescence signal associated only with changing flow conditions, denoted as $\ln ([BF]/[BF]_O)_F$, is the same for added argon as it is for added oxygen. Values used in data reduction were then determined from the relation,

$$\ln ([BF]/[BF]_O) = \ln ([BF]/[BF]_O)_M - \ln ([BF]/[BF]_O)_F. \quad (16)$$

Such corrections were not necessary for the higher temperature data nor for any of the data obtained with variable reaction zone length.

B. BF + Cl₂

Data for the rate of the reaction of BF with Cl₂ were obtained at room temperature in the flowtube geometry of Fig. 1A and over the temperature range $295 \leq T \leq 881\text{K}$ in the geometry of Fig. 1B. Higher temperature was precluded by the possibility of thermal dissociation of chlorine. All data were obtained by varying the chlorine density holding the reaction zone length fixed. Owing to the differing reaction zone lengths and differences in average gas velocity, the reaction time ranged from .012 to .065 seconds in these data. Helium was used as the inert carrier gas in geometry A, and argon was used in geometry B. At higher flow rates of argon and high flow velocity, some data were obtained which showed significant non-exponential dependence on chlorine density. It was felt that this probably was evidence of incomplete mixing of chlorine, and these data were not used in the determination of rate coefficients and are not included in Table II.

An examination of the temperature dependence of the rate constant indicates no statistically significant trend. Accordingly, the data at all temperatures were averaged together to obtain a rate constant with 95% confidence limits of

Table II. BF + Cl₂ Experiments Summary

Reaction Temperature K	Gas Flow Rates		Pressure Torr	Inert Gas	k ₂ 10 ⁻¹¹ cm ³ /molecule-sec
	10 ⁵ F _{BF₃} Std. liters/min	F _T			
295	0.50	1.2	1.6	He	1.3 ± .04
295	0.20	1.2	1.6	He	1.2 ± .03
295	0.5-1.9	5.8	8.3	He	1.3 ± .02
868	0.59	2.2	4.0	Ar	1.3 ± .06
675	0.49	2.2	4.0	Ar	1.2 ± .04
788	1.9-3.7	2.2	4.0	Ar	1.4 ± .07
881	5.2	1.5	3.1	Ar	1.5 ± .08
881	4.7	2.2	4.0	Ar	1.5 ± 0.08
295	0.0015	1.5	2.5	Ar	1.3 ± .07
295	0.018	1.5	2.5	Ar	1.3 ± .04
295	0.60	1.4	2.5	Ar	1.4 ± .04

$$k_2 = (1.4 \pm 0.2) \times 10^{-11} \text{ cm}^3/\text{molecule-sec.}$$

C. BF + NO₂

Data for the rate of the reaction of BF with NO₂ were obtained at room temperature, 294K, using the flowtube geometry of Fig. 1A. Nitrogen dioxide gas was taken from the supply cylinder and purified by trap to trap distillation. All data reported were obtained by the method of variable reactant density. The range of reaction times in these data was from .057 to .065 seconds only. As for BF + Cl₂, some non-exponential decay of BF as a function of NO₂ was evident at the highest inert gas flow rate. Again, this was attributed to incomplete mixing of reactants, and these data were not used in determining a rate coefficient. The preponderance of inert gas was argon in all experiments, but nitrogen was used as a diluent and carrier gas in the NO₂ stream.

Some special corrections were required for this reaction. Calculation of NO₂ flow rate from the measured rate of pressure decrease in the NO₂ gaseous reservoir had to account for the 2NO₂ = N₂O₄ equilibrium in the reservoir. Of greater significance was the presence of a weak fluorescence component excited by the BF resonance lamp which was independent of BF density and linear in NO₂ density. Its presence required that separate measurements be made of its intensity as a function of NO₂ density, and that the observed fluorescence be corrected for the contribution from NO₂ fluorescence.

An example of the relative magnitude of the corrections involved is presented in Fig. 8 which shows data for the relative fluorescence signal as a function of NO₂ density in the presence of BF. This figure demonstrates that

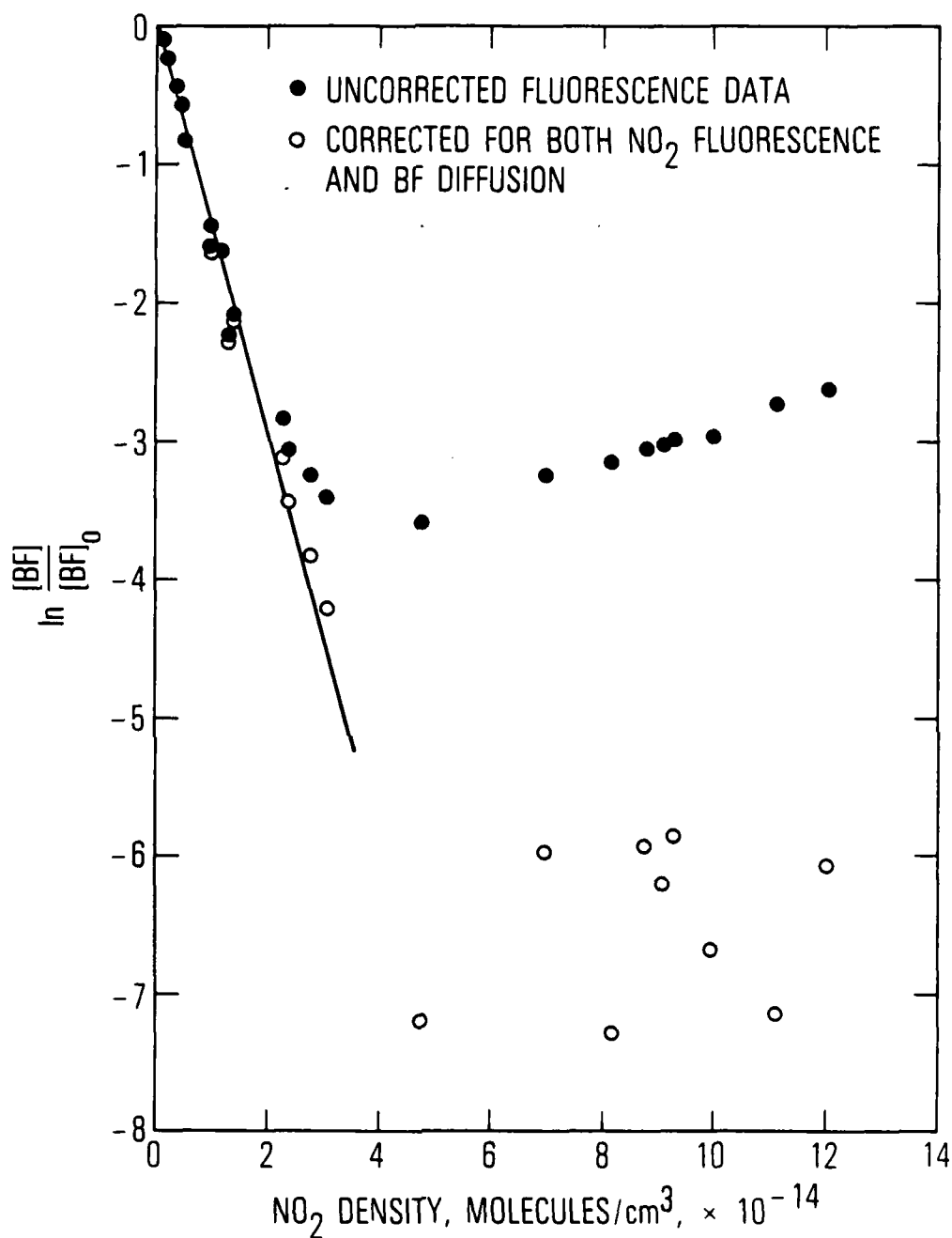


Fig. 8. Typical Uncorrected and Corrected Relative BF Fluorescence Intensity Data as a Function of NO_2 Flowtube Density. Data are shown for the third run listed in Table III. Rate coefficient for the $\text{BF} + \text{NO}_2$ reaction, $2.2 \pm 0.1 \times 10^{-13} \text{ cm}^3/\text{molecule-sec}$, was determined for this run from the slope of the straight line fit to the corrected data at the lower NO_2 densities.

some data were taken at NO₂ flow rates large enough that the contribution to total fluorescence by BF could not be reliably determined. These data were discarded in determining a rate constant. It is also clear, however, that data obtained at low NO₂ flow rates were not appreciably affected and that these data displayed a simple exponential decay. At intermediate NO₂ flow rates, corrections resulted in adjusted data which also yielded a single exponential decay rate which was the same as that obtained at lower flow rates. Only those data which were consistent with a single exponential behavior were used in deducing a rate coefficient. Rate coefficients determined from such data were independent of BF lamp intensity and independent of the flow rates of BF₃ and of inert gas. Table III presents the conditions of measurement and the deduced rate coefficient for each run. The mean value and 95% confidence limits are

$$k_3 = (2.1 \pm 0.3) \times 10^{-13} \text{ cm}^3/\text{molecule-sec.}$$

D. BF + O

No new data for the rate of this reaction are presented in this report beyond that presented in Ref. 18. Rather, it is the purpose here to present a slightly revised rate coefficient based on a recalibration of a laboratory instrument and on a slightly different analysis of the data. The instrument involved was an MKS Baratron pressure transducer. It was used as a pressure standard in the calibration of three other devices which were used in data interpretation, viz. the Bourdon tube gauge used to measure flowtube pressure, the Pace pressure transducer used to measure the rate of flow of reactant out of a reservoir of known volume, and the Matheson rotameter flowmeters used to measure other gas flow rates. In deducing a rate

Table III. BF + NO₂ Experiments Summary

Gas Flow Rates		Pressure		k ₃
10 ⁵ F _{BF₃}	Std. liters/min	F _T	Torr	10 ⁻¹³ cm ³ /molecule-sec
1.5		1.5	2.5	2.1 ± 0.1
1.1		6.1	9.3	1.9 ± 0.1
1.1		1.5	2.6	2.2 ± 0.1
1.1		1.5	2.6	2.1 ± 0.1
6.2		1.5	2.5	2.0 ± 0.1

coefficient, any errors in the calibration of the flowmeter should just cancel that for the Bourdon tube gauge, but the error in the Pace pressure transducer calibration remains. This recalibration affects only the rate of reaction of O with BF as reported in Ref. 18; all reaction rates presented herein are consistent with the new calibration.

To be consistent with the data analysis method for the other reactions reported here, the data for Reaction (4) presented in Ref. 18 were also reanalyzed by finding the best fit straight line constrained to pass through the origin in a plot of $\ln ([BF]/[BF]_0)$ vs. $([O]z/\bar{v})$. To the 95% confidence level the revised rate is

$$k_4 = (1.8 \pm 0.4) \times 10^{-10} \text{ cm}^3/\text{molecule-sec}$$

as opposed to the value of $k_4 = 1.4 \pm 0.2 \times 10^{-10}$ which was reported in Ref. 18.

E. BF + NO, SO₂, HF, H₂O, CH₃Cl, CO₂, and N₂O

No evidence of any reaction with BF was observed with a number of other reactants. This null result and an estimate of the sensitivity of the detection system to small changes in relative BF density can be used to determine upper limits to the reaction rates. These limits are not all the same for the different reactants for reasons discussed below.

1. NO

In the case of nitric oxide, fluorescence was observed in the presence of NO and in the absence of BF upon illumination by the resonance lamp. In an attempt to reduce this unwanted fluorescence, an absorption cell was placed

between the resonance lamp and the flowtube and filled with known amounts of nitric oxide at room temperature. The absorption cell was 10 cm long, and nitric oxide pressures of 10 and 50 Torr were sufficient to reduce fluorescence from NO in the flowtube by factors of ~ 30 and ~ 65 , respectively. The corresponding reduction factors in fluorescence from BF in the flowtube were 1.6 and 2.8, respectively. Despite the use of the absorption cell, no decrease in fluorescence intensity was ever observed with addition of increasing amounts of reactant NO in the presence of BF. Only an upper limit to the rate constant at room temperature can be determined:

$$k_8 < 1.5 \times 10^{-14} \text{ cm}^3/\text{molecule-sec.}$$

2. SO₂

A similar situation occurred with sulphur dioxide. As with NO, fluorescence was observed from the reactant in the absence of BF, although this fluorescence was weaker with SO₂ than with NO. Fluorescence was observed only to increase when SO₂ was added in the presence of BF, and the data provide an upper limit to the room temperature rate coefficient:

$$k_{11} < 1.5 \times 10^{-15} \text{ cm}^3/\text{molecule-sec.}$$

3. H₂O

Measurements with this reactant were made in both flowtube geometries. Measurements were first made in geometry A at $T \approx 294\text{K}$ and subsequently in geometry B at $T = 1000\text{K}$. In neither case was there any evidence for reactive removal of BF. The maximum rates implied by the absence of evidence of reaction are

$$k_5 < 4.0 \times 10^{-14} \text{ cm}^3/\text{molecule-sec at } T = 294\text{K}$$

and $k_5 < 4.0 \times 10^{-15} \text{ cm}^3/\text{molecule-sec at } T = 1000\text{K}.$

The upper limit is appreciably lower at the higher temperature only because a greater effort was made to measure a very small reaction rate.

4. HF, CH₃Cl, N₂O, and CO₂

No reaction was observed with any of these reagents. The same upper limit was established for all four reactions at room temperature:

$$k_i < 1 \times 10^{-16} \text{ cm}^3/\text{molecule-sec for } i = 6, 7, 9, \text{ or } 10.$$

F. BF + BF₃

Measurements were attempted of the rate of the reaction of BF₃ with BF. Introduction of BF₃ directly into the reaction zone caused an abrupt large decrease in fluorescence, clearly indicative of reactive removal of BF. However, subsequent removal of the BF₃ failed to cause a corresponding prompt increase in BF fluorescence. The fluorescence would recover its original value very slowly, i.e. over a period of hours. These observations suggest that BF₃ adsorbs on the walls of the flowtube, perhaps after some reaction with BF to form heavier B_xF_y species. At any rate, some boron fluoride adsorbed on the walls is clearly very effective at reactive removal of gaseous BF, and it desorbs very slowly when the BF₃ flow is discontinued.

IV. DISCUSSION

It is of interest to first discuss more fully what was measured in this study. The quantity measured was the rate of reactive removal of the molecule BF, but no measurements were made to observe the products formed. As noted earlier, Reactions (1) to (11) were written to indicate the most exothermic bimolecular product channel, but other exothermic bimolecular product channels are possible for some of these reactions. Another possibility which warrants discussion is recombination, e.g.



as opposed to Reaction (4), where M is an inert third body. As is well known, recombination can be treated as a bimolecular addition to form an energized collision complex between reactants BF and XY followed by a kinetic competition between collisional stabilization and unimolecular decomposition of the energized complex, i.e.



$$\text{with } \frac{d[\text{BFX}]}{dt} = \frac{k_{18} k_{20}}{k_{19} + k_{20} [\text{M}]} [\text{BF}] [\text{XY}] [\text{M}]. \quad (21)$$

The current studies were carried out at relatively low pressures where recombination is ordinarily unimportant. It warrants discussion in this case, however, because the very strong bonding of boron to oxygen and the halogens can cause Reaction (18) to be unusually exothermic. As a result, the energized complex lifetime, $\tau_c = k_{19}^{-1}$, can be unusually long so as to facilitate recombination, Reaction (20).

As a check on this possibility, RRKM estimates are given in Table IV for τ_c calculated from

$$\tau_c = \tau \left\{ \frac{E}{E-E_c} \right\}^s \quad (22)$$

where $\tau^{-1} = 4 \times 10^{13} \text{ sec}^{-1}$ was taken as typical of a B-F stretch in the complex. These rough estimates are based on simple classical energy density expressions which can cause serious error. However, the error should be in the direction to overestimate the collision lifetime and the rate of the recombination reaction. The range in τ_c which is listed in Table IV reflects the possible range in the parameter s of Eq. (22) which depends upon the assumed nature of the complex, i.e. loose versus tight and linear or nonlinear.

For $\text{NO}_2 + \text{BF}$, the addition complex is very short-lived because it is unstable or only marginally stable, at best, with respect to decomposition into $\text{OBF} + \text{NO}$. The other three addition complexes are relatively long-lived for such simple reagents. Nevertheless, they indicate that any recombination would be in the low pressure, termolecular limit in all three cases since $k_{19} \gg k_{20} [\text{M}]$ even for an assumed hard sphere, gas kinetic energy transfer process, $k_{hs} \sim 1.5 \times 10^{-10} \text{ cm}^3/\text{molecule-sec}$. If recombination were taking place, the rate coefficient measured here would have been linear in total

Table IV. Estimated Addition Reaction Features

Reaction	Energetics ^a $\frac{E - E_c}{E}$	Complex Lifetime ^b $-\log_{10} \tau_c$	Recombination ^c $\tau_c k_{hs}^2 [M]$
$O + BF \rightarrow OBF$	0.082	10.3-11.4	$0.2-2 \times 10^{-13}$
$O_2 + BF \rightarrow BFO_2$	0.35	10.9-11.6	$0.6-3 \times 10^{-14}$
$Cl_2 + BF \rightarrow BFCl_2$	0.16	8.8-10.0	$0.06-1 \times 10^{-11}$
$NO_2 + BF \rightarrow BFNO_2$	>0.85	~ 13	$\sim 10^{-15}$

^a $E-E_c$ is the exothermicities of Reactions (1)-(4); E is the exothermicity of the addition reaction. Estimated heats of formation of BFO_2 and $BFNO_2$ were used.

^bEstimated energized complex lifetime, calculated from Eq. (22), is given in seconds.

^c k_{hs} is an estimated hard sphere, gas kinetic rate coefficient. [M] is total number density for the highest total pressure used to study the reaction; see Table I-III and Ref. 18. The text discusses the significance of this quantity.

pressure and given by $\tau_c k_{18} k_{20} [M]$. Table IV includes entries of $\tau_c k_{hs}^2 [M]$, i.e. the largest possible value of this quantity. These upper limits are considerably below the measured values for Reactions (3) and (4), clearly indicating that reactive removal of BF by O or NO₂ was not due to recombination. For O₂ and Cl₂, however, the upper values of the ranges listed in Table IV are comparable to the measured rates. However, the absence of any dependence of the measured rate coefficients listed in Tables I and II on total pressure argues against any significant participation of recombination with O₂ or Cl₂ as well.

The failure to observe any reaction of BF with H₂O or HF is significant because addition of either of these reagents to BF should be very exothermic, e.g. $\Delta H_{298} = -346$ kJ/mole for HBF₂ formation. If formed, the lifetime of the complex could be quite long so that failure to observe any reaction suggests a slow rate for formation of the strongly bound collision intermediate. It is noteworthy²⁷ that BF₃ exhibits fast rates of association with related reagents, i.e. NH₃ and methyl amines. Thus, either BF differs from BF₃ and does not undergo a facile association reaction, or else there is some barrier preventing some initial Lewis acid-Lewis base complex from isomerizing to release the full exothermicity of the addition reaction.

In initiating this study, it was unclear what pattern of reactivity to expect from BF. On the one hand, it is isoelectronic with N₂ and CO, two reagents which react very slowly with most oxidizers. On the other hand, BF is a thermodynamically unstable specie which cannot be stored for any appreciable time at room temperature and which is capable of unusually exothermic reactions with a variety of oxidizing agents. The pattern of reactivity which has emerged places it somewhere intermediate between these very active and inactive kinetic limits. Thus, it reacts readily with some

strong oxidizing agents, viz. Cl_2 , NO_2 , and O atoms. In contrast, it reacts slowly, at best, with a variety of other reagents tested. This may be contrasted with boron atoms as an example of a very active kinetic specie. Boron atoms react very rapidly with many of these same species,¹²⁻¹⁶ viz. O_2 , H_2O , NO , and SO_2 . They also react significantly faster¹³ with N_2O and CO_2 . Although HF and CH_3Cl have not been studied, boron atoms also react rapidly^{14,16} with related compounds, viz. HCl , H_2O , and alcohols. Thus, the present results are in qualitative agreement with Timm's observation²⁰ that BF is relatively inert for a specie with such a variety of potentially exothermic reactions.

Reference 18 discusses some factors arguing for and against a simple comparison of BF reaction rates with those of the isoelectronic CO and N_2 molecules. Some properties, such as unusually large bond dissociation energies or the small polarity of the BF bond,²⁸ support an isoelectronic projection. In this regard, it is noteworthy that the rate coefficient reported¹⁷ for reaction of O_2 with BO , isoelectronic with the reactive CN radical, is considerably larger than that found here for reaction with BF , isoelectronic with CO . However, other considerations suggest that the chemical behavior of BF might be quite different from that of CO or N_2 . In particular, electronic structure calculations indicate²⁹ that individual molecular orbitals of BF are quite asymmetric so that the small overall dipole moment could be misleading.

Nevertheless, Table V presents a comparison of isoelectronic rate coefficient data. Data is not available for $\text{N}_2 + \text{NO}_2$ or Cl_2 . Indeed, the isoelectronic comparison is completely inappropriate for $\text{N}_2 + \text{Cl}_2$ because N_2Cl is not a stable molecule. The entries in the Table indicate reasonable isoelectronic trends for the O, O_2 , and Cl_2 reactions. Thus, BF and $\text{CO} + \text{Cl}_2$

Table V. Rates of Isoelectronic Reactions^a

Reaction	Exoergicity	Rate Coefficient		Ref.
	ΔH°_O	$\log_{10} A$	E^*	
$O + BF \rightarrow BO + F$	-54	-9.7	~ 0	
$O + CO \rightarrow CO + O$	0	-10.0	29	b
$O + N_2 \rightarrow NO + N$	+314	-9.9	320	c
$O_2 + BF \rightarrow OBF + O$	-89	-10.7	60	
$O_2 + CO \rightarrow CO_2 + O$	-33	-11.4	200	c
$O_2 + N_2 \rightarrow N_2O + O$	+332	-10.0	460	c
$NO_2 + BF \rightarrow OBF + NO$	-429		small	
$NO_2 + CO \rightarrow CO_2 + NO$	-226	-10.0	138	d
$Cl_2 + BF \rightarrow ClBF + Cl$	-77	-10.9	~ 0	
$Cl_2 + CO \rightarrow COCl + Cl$			$\Delta H^\circ_O + 3$	31

^aEnergies in kJ/mole. Parameters of the bimolecular rate coefficient are given as $k(\text{cm}^3/\text{molecule-sec}) = A \exp[-E^*/kT]$. Exothermicity of $CO + Cl_2$ is not available. Data on BF reactions from the current study.

^bTaken from S. Jaffe and F. S. Klein, *Trans. Faraday Soc.* **62**, 3135 (1966). See, also, T. C. Clark, S. A. Garnett, and G. B. Kistiakowsky, *J. Chem. Phys.* **52**, 4692 (1970).

^cParameters taken from the recent review of R. F. Hampson, Jr. and D. Garvin Reaction Rate and Photochemical Data for Atmospheric Chemistry 1977, NBS Special Publication 513, U.S. Dept. of Commerce (1978).

both have negligible activation energy barriers, although the $\text{CO} + \text{Cl}_2$ reaction might have an endothermicity to overcome. The available information³⁰ on this reaction actually refers to the inverse reaction. Data for O atom and O_2 molecule reactions show reasonable trends, with N_2 the least reactive and BF the most reactive with either reagent. It is also noteworthy that pre-exponential terms are approximately the same within each of these isoelectronic series. However, this isoelectronic trends picture works less well for NO_2 , with $\text{BF} + \text{NO}_2$ perhaps surprisingly fast in comparison with $\text{CO} + \text{NO}_2$. As a "pseudo-halogen," however, NO_2 might be expected to experience a stronger attractive interaction upon approach of BF as opposed to CO, and this may account for the much different reactivities.

REFERENCES

1. S. S. Cherry, L. J. van Nice, and P. I. Gold, *Pyrodynamics* 6, 275 (1968); G. S. Bahn, *Pyrodynamics* 6, 297 (1968).
2. C. W. Hand and L. K. Derr, *Inorg. Chem.* 13, 339 (1974); G. K. Anderson and S. H. Bauer, *J. Phys. Chem.* 81, 1146 (1977); P. M. Jeffers and S. H. Bauer, *Chem. Phys. Letters* 80, 29 (1981); *J. Phys. Chem.* 88, 5039 (1984).
3. S. P. Tang, N. G. Utterback, and J. F. Friichtenicht, *J. Chem. Phys.* 64, 3833 (1976).
4. U. C. Sridharan, D. L. McFadden, and P. Davidovits, *J. Chem. Phys.* 65, 5373 (1976); *ACS Symp. Ser.* 56, 136 (1977).
5. A. Brzychay, J. DeHaven, A. T. Prengel, and P. Davidovits, *Chem. Phys. Letters* 60, 102 (1978).
6. J. Dehaven, M. T. O'Connor, and P. Davidovits, *J. Chem. Phys.* 75, 1746 (1981).
7. S. M. Hosseini, J. DeHaven, and P. Davidovits, *Chem. Phys. Letters* 86, 495 (1982).
8. M. K. Bullitt, R. R. Paladugu, J. DeHaven, and P. Davidovits, *J. Phys. Chem.* 88, 4542 (1984).
9. G. J. Green and J. L. Gole, *Chem. Phys. Letters* 69, 45 (1980).
10. A. W. Hanner and J. L. Gole, *J. Chem. Phys.* 73, 5025 (1980).
11. J. L. Gole and S. A. Pace, *J. Phys. Chem.* 85, 2651 (1981).
12. U. C. Sridharan, T. G. DiGiuseppe, D. L. McFadden, and P. Davidovits, *Bull. Am. Phys. Soc.* 23, 104 (1978); *J. Chem. Phys.* 70, 5422 (1979).
13. T. G. DiGiuseppe and P. Davidovits, *J. Chem. Phys.* 74, 3287 (1981).

14. T. G. DiGiuseppe, K. Estes, and P. Davidovits, J. Phys. Chem. 86, 260 (1982).
15. R. Estes, M. B. Tabacco, T. G. DiGiuseppe, and P. Davidovits, Chem. Phys. Letters 86, 491 (1982).
16. G. C. Light and S. S. Goldberg, Bull. Am. Phys. Soc. 26, (1981).
17. I. P. Llewellyn, A. Fontijn, and M. A. A. Clyne, Chem. Phys. Letters 84, 504 (1981).
18. G. C. Light, R. R. Herm, and J. H. Matsumoto, Chem. Phys. Letters 70, 366 (1980).
19. J. Blauer, M. A. Greenbaum, and M. Farber, J. Phys. Chem. 68, 2332 (1964).
20. P. L. Timms, J. Am. Chem. Soc. 89, 1629 (1967); J. Am. Chem. Soc. 90, 4585 (1968); Advan. Inorg. Chem. Radiochem. 14, 121 (1972).
21. M. B. Moeller and S. J. Silvers, Chem. Phys. Letters 19, 78 (1973).
22. A. Fontijn and W. Felder, J. Phys. Chem. 83, 24 (1979).
23. A. A. Westenberg and N. de Hass, J. Chem. Phys. 46, 490 (1967).
24. M. S. Zahniser and M. E. Gersh, J. Chem. Phys. 75, 52 (1981).
25. R. V. Poirier and R. W. Carr, Jr., J. Phys. Chem. 75, 1593 (1971).
26. C. J. Howard, J. Phys. Chem. 83, 3 (1979).

27. See S. Glicker, J. Phys. Chem. 77, 1093 (1973) and references cited therein.
28. F. J. Lovas and D. R. Johnson, J. Chem. Phys. 55, 41 (1971).
29. P. Sutton, P. Bertommini, G. Das, T. L. Gilbert, A. C. Wahl, and O. Sinanoglu, Intern. J. Quantum. Chem. 3, 479 (1970); H. B. Jansen and P. Ros, Theoret. Chim. Acta 21, 199 (1971).
30. W. G. Burns and F. S. Dainton, Trans. Faraday Soc. 48, 39 (1952).

LABORATORY OPERATIONS

The Aerospace Corporation functions as an "architect-engineer" for national security projects, specializing in advanced military space systems. Providing research support, the corporation's Laboratory Operations conducts experimental and theoretical investigations that focus on the application of scientific and technical advances to such systems. Vital to the success of these investigations is the technical staff's wide-ranging expertise and its ability to stay current with new developments. This expertise is enhanced by a research program aimed at dealing with the many problems associated with rapidly evolving space systems. Contributing their capabilities to the research effort are these individual laboratories:

Aerophysics Laboratory: Launch vehicle and reentry fluid mechanics, heat transfer and flight dynamics; chemical and electric propulsion, propellant chemistry, chemical dynamics, environmental chemistry, trace detection; spacecraft structural mechanics, contamination, thermal and structural control; high temperature thermomechanics, gas kinetics and radiation; cw and pulsed chemical and excimer laser development including chemical kinetics, spectroscopy, optical resonators, beam control, atmospheric propagation, laser effects and countermeasures.

Chemistry and Physics Laboratory: Atmospheric chemical reactions, atmospheric optics, light scattering, state-specific chemical reactions and radiative signatures of missile plumes, sensor out-of-field-of-view rejection, applied laser spectroscopy, laser chemistry, laser optoelectronics, solar cell physics, battery electrochemistry, space vacuum and radiation effects on materials, lubrication and surface phenomena, thermionic emission, photo-sensitive materials and detectors, atomic frequency standards, and environmental chemistry.

Computer Science Laboratory: Program verification, program translation, performance-sensitive system design, distributed architectures for spaceborne computers, fault-tolerant computer systems, artificial intelligence, micro-electronics applications, communication protocols, and computer security.

Electronics Research Laboratory: Microelectronics, solid-state device physics, compound semiconductors, radiation hardening; electro-optics, quantum electronics, solid-state lasers, optical propagation and communications; microwave semiconductor devices, microwave/millimeter wave measurements, diagnostics and radiometry, microwave/millimeter wave thermionic devices; atomic time and frequency standards; antennas, rf systems, electromagnetic propagation phenomena, space communication systems.

Materials Sciences Laboratory: Development of new materials: metals, alloys, ceramics, polymers and their composites, and new forms of carbon; non-destructive evaluation, component failure analysis and reliability; fracture mechanics and stress corrosion; analysis and evaluation of materials at cryogenic and elevated temperatures as well as in space and enemy-induced environments.

Space Sciences Laboratory: Magnetospheric, auroral and cosmic ray physics, wave-particle interactions, magnetospheric plasma waves; atmospheric and ionospheric physics, density and composition of the upper atmosphere, remote sensing using atmospheric radiation; solar physics, infrared astronomy, infrared signature analysis; effects of solar activity, magnetic storms and nuclear explosions on the earth's atmosphere, ionosphere and magnetosphere; effects of electromagnetic and particulate radiations on space systems; space instrumentation.

...

END

DTIC

6-86